Image Denoising Algorithm with a Three-dimensional Grid System of Coupled Nonlinear Elements

Atsushi Nomura[1], Yoshiki Mizukami[2] and Koichi Okada[3]

[1]*Faculty of Education, Yamaguchi University, Yoshida 1677-1, Yamaguchi 753-8513, Japan*

[2]*Graduate School of Science and Engineering, Yamaguchi University, Tokiwadai 2-16-1, Ube 755-8611, Japan*

[3]*Center for the Promotion of Higher Education, Yamaguchi University, Yoshida 1677-1, Yamaguchi 753-8511, Japan*

Keywords: FitzHugh-Nagumo, Coupled Nonlinear Elements, Three-dimensional Grid, Reaction-diffusion, ODE.

Abstract: This paper presents an image denoising algorithm with a three-dimensional grid system of coupled nonlinear elements. The system consists of a two-dimensional image grid and a one-dimensional grid representing a quantized image brightness. At each grid point, a FitzHugh-Nagumo type nonlinear element is placed and coupled with other elements placed at its nearest neighboring grid points. The FitzHugh-Nagumo element is described with a set of time-evolving ordinary differential equations, and is tuned to be excitable. When we externally stimulate the grid system with an image brightness distribution, we could observe that noise in the distribution was reduced and signal was strengthened as time proceeds. Thus, the image denoising algorithm utilizes this property of the grid system, in which we propose to modify external stimuli so as to have broad Gaussian distributions. We confirm performance of the algorithm on artificial and real images in comparison with two classical algorithms of a diffusion equation and median filtering.

1 INTRODUCTION

Gaussian filtering is a classical and elementary technique for smoothing and denoising in image processing and computer vision (Gonzalez and Woods, 1992). We convolve a Gaussian function with an image brightness distribution, and obtain its blurred or smoothed distribution. A diffusion equation gives the mathematically equal result with Gaussian filtering (Koenderink, 1984). This is because a solution of the diffusion equation is expressed by a convolution of a Gaussian function with its initial condition.

There is a trade-off between reducing image noise and preserving image structures. If we try to reduce noise with a Gaussian function having a large spatial spread, we shall obtain much smoothed or fully denoised image. However, at the same time Gaussian filtering removes detailed structures of the image such as edges and feature points. Thus, image denoising algorithms are required to reduce noise as well as to preserve detailed image structures.

Perona and Malik proposed an image processing algorithm utilizing a diffusion equation, in which its diffusion coefficient is anisotropic and is modulated according to a gradient of an image brightness distribution (Perona and Malik, 1990; Mrázek and Navara,

2003). They intended to prevent over-smoothing across image edges. Tomasi and Manduchi proposed an extension of Gaussian filtering, named 'bilateral filtering' (Tomasi and Manduchi, 1998), which includes geometric closeness and photometric similarity as the kernel of Gaussian filtering; the classical Gaussian filtering relies on only the geometric closeness. A nonlocal means algorithm (Buades et al., 2010) is another extension of Gaussian filtering; the novel point of the algorithm is to utilize windows having brightness patterns similar to that of a target window.

There are several image denoising approaches such as median filtering (Gonzalez and Woods, 1992; Eng and Ma, 2001), a total variation approach (Guo et al., 2011) and a nonlocal approach (Buades et al., 2010; Dabov et al., 2007; Katkovnik et al., 2010). The median filtering constructs a histogram on image brightness in a local area, and chooses a middle brightness level as its representative. The total variation approach defines a functional taking account of noise property, derives a Euler-Lagrange type reaction-diffusion equation, and numerically solves the equation. The nonlocal approach was developed from the idea of the nonlocal means algorithm (Buades et al., 2010); see also the review ar-

ticles (Buades et al., 2010; Katkovnik et al., 2010).

Nomura et al. (2012) proposed a stereo algorithm with a three-dimensional grid system of coupled nonlinear elements. The algorithm successfully reconstructs a disparity distribution in the three-dimensional grid system of the elements externally stimulated by a similarity measure between stereo images. In the algorithm, they placed a FitzHugh-Nagumo type nonlinear excitable element at each grid point, and coupled neighboring elements. The three-dimensional grid system approximates to a three-dimensional FitzHugh-Nagumo type reaction-diffusion system (FitzHugh, 1961; Nagumo et al., 1962); a one-dimensional version of the system describes a pulse propagation phenomenon along nerve axon, and has a biological background.

Inspired by the previous stereo algorithm (Nomura et al., 2012) having the biological background, we propose an image denoising algorithm with the isotropic three-dimensional grid system of coupled FitzHugh-Nagumo nonlinear excitable elements. The novel point of the proposed algorithm lies in the manner of externally stimulating the elements in comparison with the previous stereo algorithm. We apply the algorithm and two other classical ones to artificial and real images, and confirm their quantitative performance.

2 THE ALGORITHM

2.1 FitzHugh-Nagumo Element

A FitzHugh-Nagumo element is described with a set of equations having two variables of an activator $u(t)$ and an inhibitor $v(t)$ (FitzHugh, 1961; Nagumo et al., 1962), as follows:

$$\frac{\mathrm{d}u}{\mathrm{d}t} = f(u,v) + \mu S = \frac{1}{\varepsilon}[u(u-a)(1-u) - v] + \mu S,$$
(1)

$$\frac{\mathrm{d}v}{\mathrm{d}t} = g(u,v) = u - bv,$$
(2)

in which a and b are constants controlling the stability characteristic of the element, and ε is a small constant $(0 < \varepsilon \ll 1)$; S is an external stimulus and μ is its coefficient. Depending on the parameter settings of a, b and ε under $\mu S = 0$, the element becomes mono-stable or bi-stable, as shown in Fig. 1. For example, the element becomes bi-stable in the case of $a = 0.3$ and $b = 10$; any solution (u,v) converges to either of the stable points A or B. An excited state refers to the area having $u \simeq 1$ around B, and a resting state refers to the area having $u \simeq 0$ around A. We can roughly
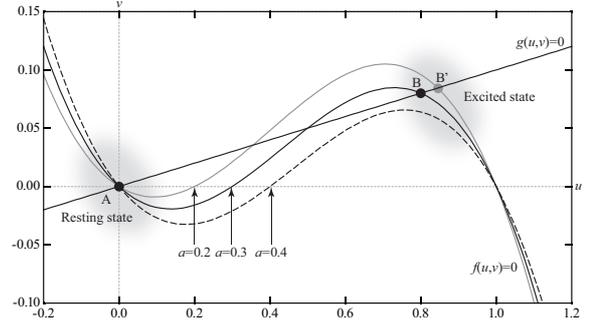
Figure 1: Null-clines of $f(u,v) = g(u,v) = 0$ in a FitzHugh-Nagumo type nonlinear element of Eqs. (1) and (2) with $a = 0.2, 0.3, 0.4$, the fixed $b = 10$ and $\mu S = 0$. The element has stable steady states denoted by A, B and B', depending on the parameter settings; it becomes bi-stable in the cases of $a = 0.2, 0.3$, and mono-stable in that of $a = 0.4$. An excited state refers to the area having $u \simeq 1$ around B and B', and a resting state refers to the area having $u \simeq 0$ around A.

explain that the parameter a in Eq. (1) is a threshold level for dividing a state of an element into either of an excited state or a resting state under the constraint of $v = 0$.

2.2 Coupled Elements in a Three-dimensional Grid

Let $I_{i,j}$ be image brightness observed at a point (i, j) on an image grid X × Y. The image brightness is quantized into $(N + 1)$ gray levels Z = $\{0, 1, \cdots, N\}$. Images should satisfy two constraints: uniqueness and continuity. The uniqueness constraint requires that a particular image point (i, j) has only one brightness level $I_{i,j}$. The continuity constraint assumes that neighboring points have the same or similar brightness levels except for boundaries of brightness patterns. These constraints are similar to those of the stereo vision problem (Nomura et al., 2012). Randomly distributing noise does not satisfy the continuity constraint; an algorithm with the two constraints is expected to reduce random noise.

A three-dimensional grid system utilized here consists of $(i, j, k) \in$ X × Y × Z, in which coupled FitzHugh-Nagumo type nonlinear elements having $(u_{i,j,k}, v_{i,j,k})$ are placed at the grid points according to the manner of Nomura et al. (2012), as follows:

$$\frac{\mathrm{d}u_{i,j,k}}{\mathrm{d}t} = C_u \left[\overline{u}\big|_{i,j,k} - 6u_{i,j,k} \right] + f(u_{i,j,k}, v_{i,j,k}, a_{i,j,k}) + \mu S_{i,j,k},$$
(3)

$$\frac{\mathrm{d}v_{i,j,k}}{\mathrm{d}t} = C_v \left[\overline{v}\big|_{i,j,k} - 6v_{i,j,k} \right] + g(u_{i,j,k}, v_{i,j,k}),$$
(4)

in which

$$\overline{u}|_{i,j,k} = \sum_{(i',j',k')\in\ell} u_{i+i',j+j',k+k'}$$

with

$$\ell = \{(-1,0,0),(1,0,0),(0,-1,0),(0,1,0),(0,0,-1),(0,0,1)\}.$$

Note that the neighboring elements are coupled via both of the activator and inhibitor variables.

A system of the coupled elements has a property in which an excited state propagates into its neighboring areas. Thus, we can expect that an area stimulated by positive $\mu S_{i,j,k}$ becomes an excited state and extends into its neighboring areas over noise; this property works for the continuity constraint. For image denoising, the system needs to satisfy the uniqueness constraint, which allows each grid point (i,j) to have only one brightness level. If a grid point (i,j,k) has already reached an excited state, the other grid points (i,j,k'), $k' \in Z \setminus \{k\}$, at the same image grid point (i,j) must be inhibited to reach excited states; $Z \setminus \{k\}$ denotes a set of grid points excluding the point k in Z. Let us recall that the parameter a in Eq. (1) is the threshold level which divides a state of an element into an excited state or a resting state. Thus, we do not fix the parameter a, but modulate the parameter depending on states of other grid points (i,j,k'), $k' \in Z \setminus \{k\}$, as follows:

$$a_{i,j,k} = A_0 + \frac{A_2 - A_0}{2}$$
$$\times \left[1 + \tanh\left(\max_{k' \in Z \setminus \{k\}} u_{i,j,k'} - A_1 \right) \right], \quad (5)$$

in which A_0, A_1 and A_2 are constants and Eq. (5) is monotonically increasing.

A system of diffusively coupled FitzHugh-Nagumo elements, that is, a set of FitzHugh-Nagumo type reaction-diffusion equations simulates a pulse propagation phenomenon observed along a nerve axon (FitzHugh, 1961; Nagumo et al., 1962); the pulse propagation is stable, even if there is a little noise on the nerve axon. Thus, a set of Eqs. (3) and (4) with a fixed $a_{i,j,k} = a$ and the first order neighborhood ℓ roughly approximates to the FitzHugh-Nagumo type reaction-diffusion equations, and has the biological background of the pulse propagation.

In addition, by imposing the condition of $f(u_{i,j,k}, v_{i,j,k}) = g(u_{i,j,k}, v_{i,j,k}) = S_{i,j,k} = 0$ on Eqs. (3) and (4), we obtain an approximated discrete version of two diffusion equations. An algorithm of Gaussian filtering is realized with a two-dimensional version of either Eqs. (3) or (4) under the condition.

Temporal discretization of Eqs. (3) and (4) provides a set of linear equations. With appropriate initial conditions and boundary ones on the two variables
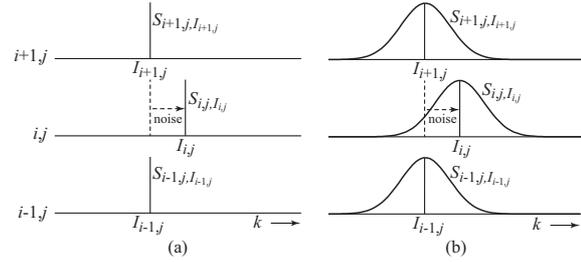
Figure 2: External stimuli $S_{i,j,k}$ for the proposed algorithm in a situation of a noise-perturbed image brightness distribution $I_{i,j}$; the image brightness $I_{i,j}$ is perturbed with a noise at an image point (i,j). Figure (a) shows three external stimuli with $S_{i-1,j,k} = \delta(k - I_{i-1,j}), S_{i,j,k} = \delta(k - I_{i,j})$ and $S_{i+1,j,k} = \delta(k - I_{i+1,j})$, in which $\delta(\cdot)$ denotes the delta function. Figure (b) shows three external stimuli proposed with Eq. (6).

$(u_{i,j,k}, v_{i,j,k})$, we can numerically compute temporal developments of the two variables.

2.3 External Stimuli

Now, we propose a manner of externally stimulating each element in the grid system. Let us consider a situation in which an image point is perturbed with noise and its surrounding points are not. If the delta function is employed as $S_{i,j,k} = \delta(k - I_{i,j})$, the noise prevents two adjacent image grid points with the same brightness level from strengthening each other through Eq. (3), as shown in Fig. 2(a). Thus, this paper proposes to employ the following external stimulus

$$S_{i,j,k} = \exp\left(-\frac{(k - I_{i,j})^2}{\sigma^2} \right) \quad (6)$$

so as to give the stimulus more widely along the k-direction as shown in Fig. 2(b); σ in Eq.(6) denotes the width of the Gaussian.

Initial conditions for $u_{i,j,k}$ and $v_{i,j,k}$ are set to zero at all points $(i,j,k) \in X \times Y \times Z$. A zero-gradient boundary condition governs borders of the grid system $X \times Y \times Z$.

After finite duration of time $(0 < t \le L_t)$, the algorithm creates a denoised image

$$I_{i,j}^* = \underset{k \in Z}{\text{argmax}}\, u_{i,j,k} \quad (7)$$

Algorithm 1 gives a pseudo code of the algorithm.

3 EXPERIMENTAL RESULTS

We applied three image denoising algorithms to artificial and real images, and evaluated their results. The three algorithms were as follows: the proposed algo-
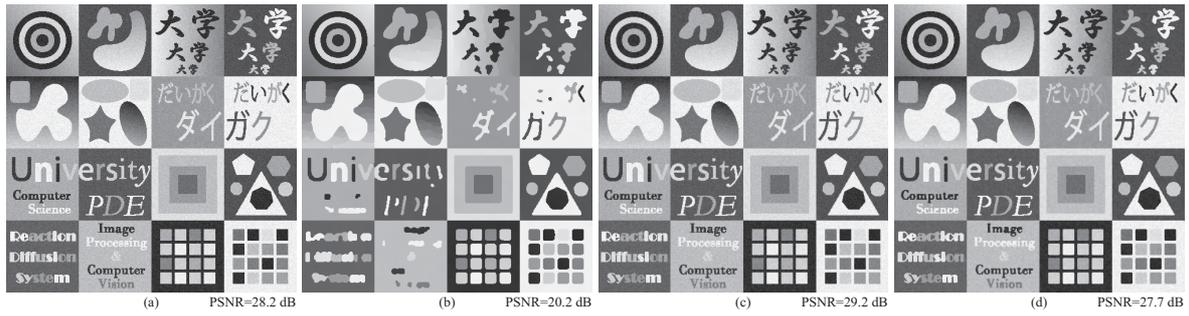
Figure 3: Experimental results of image denoising with the proposed algorithm, a diffusion algorithm and median filtering on an artificial image. Figure (a) shows the artificial image (500×500 pixels and 256 brightness levels) with an additive Gaussian noise of the standard deviation 10 and zero-average [see Ref. (Nomura et al., 2011) for the original artificial image without noise]. Figure (b) shows a result obtained by the proposed algorithm at $t = 10$ with the parameter setting of $C_u = 25, C_v = 100, A_0 = 0.07, A_1 = 0.7, A_2 = 0.5, b = 10, \varepsilon = 1.0 \times 10^{-2}, \Delta t = 1/100$ and $\sigma = 10$. Figure (c) shows a result obtained by the diffusion algorithm at $t = 0.04$ with the parameter setting of $C_u = 2.5$ and $\Delta t = 1/100$. Figure (d) shows a result obtained by the median filtering with a local area of 5×5 pixels. Each figure has a value evaluated by the measure PSNR.
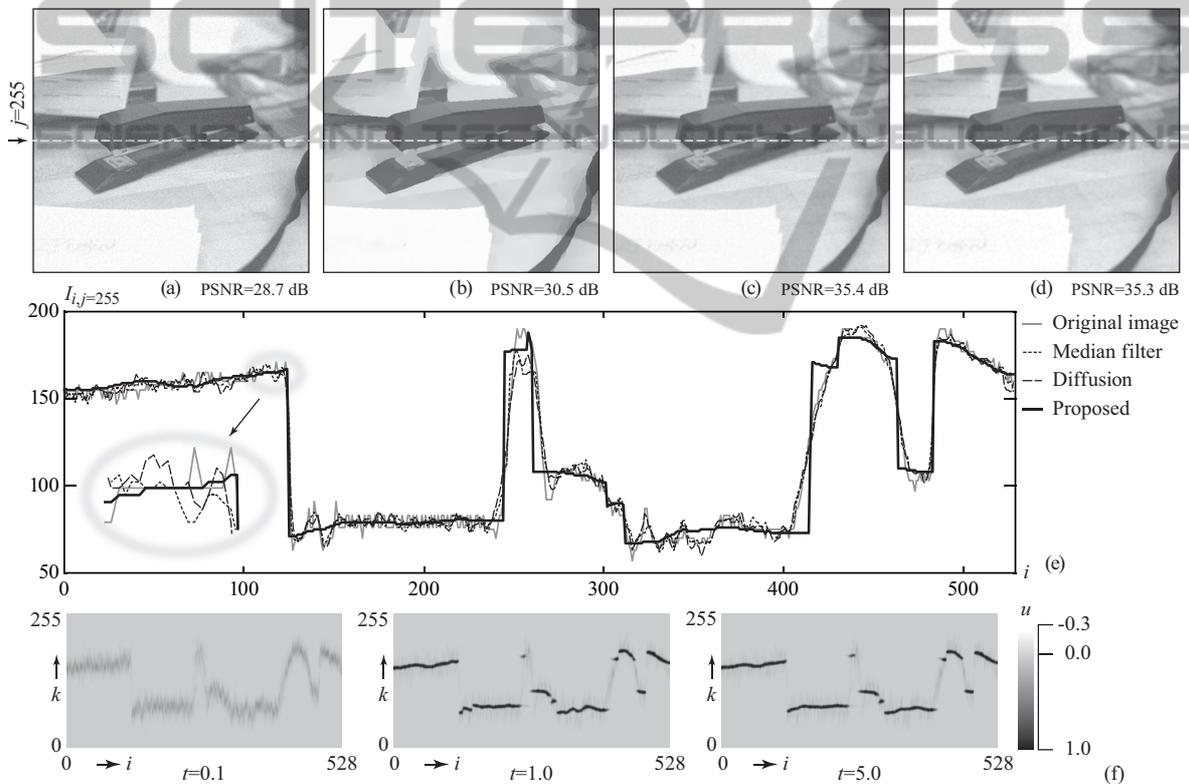
Figure 4: Experimental results of image denoising with the proposed algorithm, a diffusion algorithm and median filtering on a real image provided on a website (Heath et al., 2014). Figure (a) shows the real image (529×510 pixels and 256 brightness levels) with an additive Gaussian noise of the standard deviation 10 and zero-average. Figure (b) shows a result obtained by the proposed algorithm at $t = 10$ with the same parameter setting as that of Fig. 3(b). Figure (c) shows a result obtained by the diffusion algorithm at $t = 0.24$ with the same parameter setting as that of Fig. 3(c). Figure (d) shows a result obtained by the median filtering with a local area of 3×3 pixels. Each of Figs. (a)~(d) has a value evaluated by the measure PSNR. Figure (e) shows one-dimensional profiles $I_{i,j=255}$ of the brightness distributions of the original image and the results shown in Figs. (b)~(d); the profiles around $i = 110$ are enlarged for more detailed confirmation. Figure (f) shows temporal developments of a two-dimensional distribution $u_{i,j=255,k}$ obtained at $t = 0.1, 1.0, 5.0$ by the proposed algorithm; a gray level shows the distribution $u_{i,j=255,k}$, and thus black areas indicate excited states of elements. The maximum value at each image point (i, j) along the direction k is chosen, and its k value denotes the brightness level of the denoised image [see Eq. (7)].

Algorithm 1 : Proposed image denoising algorithm, in which Eqs. (3) and (4) are discretized with a finite time-difference Δt for their numerical computation.

1: **for all** $(i,j) \in X \times Y$ **do**
2:      **for all** $k \in Z$ **do**
3:          $S_{i,j,k} \leftarrow \exp\left(-\frac{(k-I_{i,j})^2}{\sigma^2}\right)$ ▷ Eq.(6)
4:          $u_{i,j,k}^{n=0} \leftarrow 0, v_{i,j,k}^{n=0} \leftarrow 0$ ▷ Initial conditions.
5:      **end for**
6: **end for**
7: $n \leftarrow 0$
8: **while** $n < L_t/\Delta t$ **do**
9:      **for all** $(i,j,k) \in X \times Y \times Z$ **do**
10:          Compute $u_{i,j,k}^{n+1}, v_{i,j,k}^{n+1}$.   ▷ Eqs. (3)$\sim$(5)
11:      **end for**
12:      $n \leftarrow n+1$
13: **end while**
14: **for all** $(i,j) \in X \times Y$ **do**
15:      $I_{i,j}^* \leftarrow \underset{k \in Z}{\arg\max}\, u_{i,j,k}^n$ ▷ Eq. (7)
16: **end for**

rithm, a diffusion algorithm and median filtering. The diffusion algorithm utilizes a simple diffusion equation with the initial condition of an image brightness distribution. The median filtering has a local area in which the median of brightness values is chosen as the representative brightness value (Gonzalez and Woods, 1992).

The following peak-signal-to-noise-ratio (PSNR) evaluates image quality, as follows:

$$\text{PSNR} = 10\log_{10}\left[\frac{N^2|X \times Y|}{\sum_{(i,j)\in X \times Y}(I_{i,j}^t - I_{i,j}^o)^2}\right] \ [\text{dB}],$$
$$(8)$$

in which $I_{i,j}^t$ denotes the original image without noise, $I_{i,j}^o$ denotes an image for quality assessment, and $|X \times Y|$ denotes the image size.

Figure 3 shows results of image denoising on an artificial image with an additive Gaussian noise. According to the measure PSNR, the diffusion algorithm achieved the best performance of 29.2 dB, which is better than the level of PSNR = 28.2 dB measured on the input image, and performance of the other two algorithms was worse than the level of the input image.

Figure 4 shows results of image denoising on an image generated by adding a Gaussian noise to a real photo image (Heath et al., 2014). According to the measure PSNR, the two algorithms of the diffusion algorithm and the median filtering achieved almost the same performance of about 35 dB, and the proposed algorithm gave 30.5 dB which is better than the quality of the input image 28.7 dB of Fig. 4(a). For more detailed confirmation on the re-
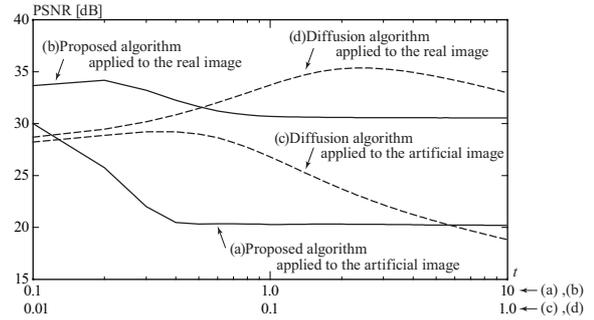
Figure 5: Image denoising processes evaluated by the measure PSNR. Curves (a) and (b) show results of the proposed algorithm applied to the artificial and real images (see Figs 3 and 4). Curves (c) and (d) show results of the diffusion algorithm applied to the same artificial and real images; the algorithm achieved the best performance at $t = 0.04$ on the artificial image, and at $t = 0.24$ on the real image. Note that a time scale for (a) and (b) is different from that for (c) and (d).

sults, Fig. 4(e) shows one-dimensional profiles of image brightness distributions at the center ($j = 255$) in the images of Figs. 4(a)$\sim$(d). Figure 4(f) shows the temporal developments of a two-dimensional distribution $u_{i,j=255,k}$, $(i,k) \in X \times Z$ obtained at three different time instances.

Figure 5 shows temporal changes of the measures PSNR evaluating image denoising processes of the proposed algorithm and the diffusion one. The measures show that the algorithm mostly converged at $t = 1.0$ on both the artificial and real images, and the diffusion algorithm did not converged in the range of $0 < t \leq 10$.

Let us discuss the above experimental results. The proposed algorithm reduced noise with preserving edges, as shown around $i = 110 \sim 120$ in Fig. 4(e). Fig. 4(f) demonstrates the process in which the algorithm dynamically connected neighboring areas on the $i-k$ grid. In contrast to these successful results, the proposed algorithm failed to preserve image details in Fig. 3(b), and created step-wise brightness distributions in the areas having high gradients in image brightness distributions, for example, as shown around $i = 410$ in Fig. 4(e). Figure 4(f) shows that the proposed algorithm failed to obtain continuity in the corresponding high gradient areas of the brightness. We need to develop the algorithm so as to preserve image details and simultaneously to support the continuity in the high gradient areas; we believe that how to choose the width σ adaptively is a key point to solve these problems.

Performance of the diffusion algorithm highly depends on the stopping time, as shown in Fig. 5; this is known as the stopping time evaluation prob-

lem (Mrázek and Navara, 2003). The proposed algorithm converges in enough duration of time. This is because the FitzHugh-Nagumo type nonlinear excitable element has one or two stable steady state(s), and convergence of the uncoupled element is guaranteed (Murray, 1989).

4 CONCLUSION

This paper presented an image denoising algorithm, which consists of a three-dimensional grid system of coupled FitzHugh-Nagumo type nonlinear excitable elements. In particular, each element is externally stimulated so as to fit the grid system to the task of image denoising. The PSNR measure evaluated performance of the algorithm in comparison with the two other classical algorithms of a diffusion equation and median filtering on artificial and real images. As the results, although the overall performance of the proposed algorithm did not achieve that of the other ones, it successfully recovered image brightness distributions around edges as well as reducing noise. We believe that this is a merit of the proposed algorithm having nonlinearlity in comparison with the other ones. The convergence of the proposed algorithm was numerically confirmed.

ACKNOWLEDGEMENTS

REFERENCES

Buades, A., Coll, B., and Morel, J. M. (2010). Image denoising methods. A new nonlocal principle. *SIAM Review*, 52:113–147.

Dabov, K., Foi, A., Katkovnik, V., and Egiazarian, K. (2007). Image denoising by sparse 3-d transform-domain collaborative filtering. *IEEE Transactions on Image Processing*, 16:2080–2095.

Eng, H.-L. and Ma, K.-K. (2001). Noise adaptive soft-switching median filter. *IEEE Transactions on Image Processing*, 10:242–251.

FitzHugh, R. (1961). Impulses and physiological states in theoretical models of nerve membrane. *Biophysical Journal*, 1:445–466.

Gonzalez, R. C. and Woods, R. E. (1992). *Digital Image Processing*. Addison-Wesley, New York, USA.

Guo, Z., Liu, Q., Sun, J., and Wu, B. (2011). Reaction-diffusion systems with p(x)-growth for image denoising. *Nonlinear Analysis: Real World Applications*, 12:2904–2918.

Heath, M., Sarkar, S., Sanocki, T., and Bowyer, K. (confirmed on June 1st, 2014). Edge detector comparison. Available from: http://marathon.csee.usf.edu/edge/edge_detection.html.

Katkovnik, V., Foi, A., Egiazarian, K., and Astola, J. (2010). From local kernel to nonlocal multiple-model image denoising. *International Journal of Computer Vision*, 86:1–32.

Koenderink, J. J. (1984). The structure of images. *Biological Cybernetics*, 50:363–370.

Mrázek, P. and Navara, M. (2003). Selection of optimal stopping time for nonlinear diffusion filtering. *International Journal of Computer Vision*, 52:189–203.

Murray, J. D. (1989). *Mathematical Biology*. Springer-Verlag, Berlin, Germany.

Nagumo, J., Arimoto, S., and Yoshizawa, S. (1962). An active pulse transmission line simulating nerve axon. *Proceedings of the IRE*, 50:2061–2070.

Nomura, A., Ichikawa, M., Okada, K., Miike, H., and Sakurai, T. (2011). Edge detection algorithm inspired by pattern formation processes of reaction-diffusion systems. *International Journal of Circuits, Systems and Signal Processing*, 5:105–115.

Nomura, A., Okada, K., Mizukami, Y., Miike, H., Ichikawa, M., and Sakurai, T. (2012). Subpixel stereo disparity for surface reconstruction by utilising a three-dimensional reaction-diffusion system. In *Proceedings of the 27th Image and Vision Computing New Zealand Conference*, pages 144–149, Dunedin, New Zealand.

Perona, P. and Malik, J. (1990). Scale-space and edge detection using anisotropic diffusion. *IEEE Transactions on Pattern Analysis and Machine Intelligence*, 12:629–639.

Tomasi, C. and Manduchi, R. (1998). Bilateral filtering for gray and color images. In *Proceedings of the 1998 IEEE International Conference on Computer Vision*, pages 839–846, Bombay, India.